



Contents lists available at ScienceDirect

Journal of King Saud University – Science

journal homepage: www.sciencedirect.com

Original article

Synthesis of gold nanoparticles using bacterial cellulase and its role in saccharification and bioethanol production from aquatic weeds

Chirom Aarti^{a,*}, Ameer Khusro^a, Paul Agastian^a, Palaniselvam Kuppusamy^b, Dunia A. Al Farraj^c^a Research Department of Plant Biology and Biotechnology, Loyola College (Affiliated to University of Madras), Nungambakkam, Chennai 600034, Tamil Nadu, India^b Department of Animal Biotechnology, Jeonbuk National University, Jeonju 54896, South Korea^c Department of Botany and Microbiology, College of Science, King Saud University, P.O. 2455, Riyadh 11451, Saudi Arabia

ARTICLE INFO

Article history:

Received 29 December 2021

Revised 6 March 2022

Accepted 11 March 2022

Available online 22 March 2022

Keywords:

Aquatic weeds

Bioethanol

Biofuel

Cellulase

Gold nanoparticles

Saccharification

ABSTRACT

In this investigation, gold nanoparticles (AuNPs) were synthesized using cellulase (partially purified from *Glutamicibacter arilaitensis* strain ALA4) as reducing agent. The biosynthesis of AuNPs was confirmed by observing the appearance of purple colour solution with surface plasmon resonance absorption peak (λ_{\max}) at 574 nm. The SEM analysis showed the synthesis of gold nanocrystals with an average size of 5–7 nm. Cellulase was partially purified from strain ALA4 using standard protocols, and further immobilized on AuNPs for assessing its role in the saccharification of alkali (4% w/v NaOH) pre-treated aquatic weeds (*Alternanthera philoxeroides* and *Brachiaria mutica*) biomass. The pre-treated biomass of *A. philoxeroides* exhibited maximum total reducing sugar (TRS) yield of 18.95 ± 0.18 mg/g at 72 h. The pre-treated biomass exhibited increased saccharification degree of 38.25 ± 0.8 , 49.05 ± 0.7 , 67.05 ± 0.7 , 85.27 ± 0.8 , and $67.99 \pm 0.8\%$ from 12 to 96 h. Likewise, the pre-treated biomass of *B. mutica* exhibited maximum TRS yield of 20.98 ± 0.17 mg/g at 72 h. The pre-treated biomass exhibited increased saccharification degree of 44.46 ± 0.7 , 55.53 ± 0.8 , 73.26 ± 0.7 , 94.41 ± 0.8 , and $73.3 \pm 0.7\%$ from 12 to 96 h. Bioethanol production from pre-treated aquatic weeds were estimated by simultaneous saccharification and fermentation process using yeast cells immobilized on sodium alginate. Ethanol content was estimated using Gas Chromatography. The yeast cells immobilized in calcium alginate beads showed ethanol production of 45.09 and 50.1% from NaOH pre-treated *A. philoxeroides* and *B. mutica* biomass, respectively. Findings of this study suggested pronounced role of bacterial cellulase-assisted-synthesized AuNPs in biofuel industries for the successful production of bioethanol from distinct aquatic weeds biomass in a cost-effective manner in future.

© 2022 The Author(s). Published by Elsevier B.V. on behalf of King Saud University. This is an open access article under the CC BY license (<http://creativecommons.org/licenses/by/4.0/>).

1. Introduction

No doubt, enzymatic hydrolysis of lignocellulosic biomass is considered as a more effectual approach than other hydrolysis techniques (Aarti et al., 2018). In fact, enzymes exhibit higher specificity and catalytic action as compared to the other catalysis mechanisms (Reynaldo et al., 2018). Currently, certain enzymes such as cellulases, amylases, xylanases, and hemicellulases are available commercially and they have almost completely replaced

chemical-based hydrolysis of lignocellulosic biomasses (Chukwuma et al., 2020). However, the high cost of enzyme productivity is the leading concern of biofuel industries at present. Thus, in order to maintain the biomass hydrolysis process economical, a new strategy is certainly required (Justine et al., 2021).

Over the past decade, the applications of nanobiotechnology have extended broadly in diversified areas of science and technology such as wastewater treatment, removal of contaminants from water, drug delivery, biomedicine, biosensors, bioremediation, fabrics, cosmetics, and coating (Shah et al., 2010; Kanimozhi et al., 2018; Al-Dhabi et al., 2019; Kanimozhi et al., 2019; Nalini et al., 2019; Arasu et al., 2019; Khusro et al., 2020; Agayeva et al., 2020; Judy et al., 2021). The utilization of nanomaterials in bioenergy sectors for lignocellulosic biomass hydrolysis, followed by bioethanol productions has attracted immense attention of worldwide researchers (Aarti et al., 2021). Nanoparticles help enhance not only the pre-treatment efficiency of biomass, enzymatic

* Corresponding author.

E-mail address: aartichirom@gmail.com (C. Aarti).

Peer review under responsibility of King Saud University.



Production and hosting by Elsevier

hydrolysis, and reaction rate but also improve the productivity (Cherian et al., 2015). Magnetic nanoparticles, nickel nanoparticles, iron nanoparticles, cobalt nanoparticles, silver nanoparticles, and silicon nanoparticles are being extensively used to immobilize hydrolytic enzymes for bioethanol production from lignocellulosic biomass (Singhvi and Kim, 2020). Nanoparticles may induce catalytic efficiency through the increased enzyme loading due to larger surface area (Cherian et al., 2015). Surprisingly, the role of gold nanoparticles (AuNPs) in the saccharification of lignocellulosic biomass is not investigated yet.

Gold nanoparticles represent exemplary interest because of its intrinsic characteristics. The AuNPs show strong optical absorption and scattering extending from the visible to near-infrared spectrum (Jayakumar et al., 2018; Lydia et al., 2020). Additionally, size- and shape-dependent optical properties, large surface-to-volume ratio, prominent biocompatibility, enhancing mass transfer, reusability, and reduced toxicity are unique characteristics of AuNPs which makes them pivotal nanomaterial in nanobiotechnology (Pandit et al., 2022). In addition, chemical stability and tunable geometry suggest the preference of AuNPs over other metallic nanoparticles. Previous studies have reported the wide applications of AuNPs in drug-delivery, photo-thermal therapy, imaging, sensing, catalysis, and bioremediation of toxic chemicals (Akintelu et al., 2021; Sathiyaraj et al., 2021). Surprisingly, its role in the biofuel industries is very limited.

Considering the numerous benefits of nanoparticles-mediated enzymes catalysis viz. improving the production of simple sugar as well as bioethanol yield (Singhvi and Kim, 2020) and gap of the AuNPs research in biofuel industries, this study was aimed not only to synthesize AuNPs using partially purified cellulase of *Glutamicibacter arilaitensis* strain ALA4 (a soil isolate) but also evaluate the role of immobilized cellulase (on AuNPs) in the saccharification ability, followed by bioethanol production from pre-treated aquatic weeds biomass.

2. Materials and methods

2.1. Chemicals and glassware

Tetrachloroauric acid ($\text{HAuCl}_4 \cdot 3\text{H}_2\text{O}$) was obtained from Sigma-Aldrich, India. All the sterilized glasswares were rinsed with sterile double-distilled water. All chemicals, reagents, and solvents used in this investigation were of the highest purity, and were obtained from HiMedia, India.

2.2. Bacterium of interest

G. arilaitensis strain ALA4, isolated previously from soil sample, was used in this investigation (Aarti et al., 2017).

2.3. Reducing agent preparation

The partially purified cellulase (1 mg/mL) from strain ALA4, as described in our previous report (Aarti et al., 2022) was dissolved in sodium phosphate buffer (1 M, pH – 7.0), and was used as reductant.

2.4. Synthesis of AuNPs using cellulase

The ability of cellulase to synthesize AuNPs was determined by mixing cellulase and 1 mM $\text{HAuCl}_4 \cdot 3\text{H}_2\text{O}$ solution in a ratio of 1:1 in a clean glass vial. The vial was kept in the centre of microwave oven (1050 W, 2450 MHz) and irradiated for 30 s. During the heating mechanism, the colourless solution was changed into dark purple colour, thereby representing the synthesis of AuNPs.

2.5. Characterization of AuNPs

The biosynthesis of AuNPs was further characterized by UV-Vis spectroscopy (400–800 nm), Fourier transform-infrared (FT-IR) spectroscopy, zeta potential analyzer, particle size analyzer (Dynamic light scattering or DLS analysis), diffractometer (X-ray Diffraction or XRD), Energy-Dispersive X-ray (EDX) spectroscopy, and scanning electron microscopy (SEM) using standard protocols.

2.6. Cellulase immobilization on AuNPs

The immobilization of cellulase on AuNPs was carried out as per the methodology of Mishra and Sardar (2015) with slight modifications. Cellulase (1 mg/mL) was added into AuNPs solution and incubated at 25 °C for 1 h under constant shaking. After required incubation period, the solution was centrifuged at 10,000 g for 10 min at 4 °C. Further, AuNPs constituting adsorbed cellulase was washed with sodium acetate buffer (50 mM; pH – 5.0) containing 1 M NaCl in order to remove the loosely bound cellulase.

2.7. Saccharification of aquatic weeds using cellulase immobilized on AuNPs-

2.7.1. Pre-treatment of aquatic weeds

Two aquatic weeds - *Alternanthera philoxeroides* (Alligator weed) and *Brachiaria mutica* (Para grass) were used in this study. *A. philoxeroides* and *B. mutica* were collected from Thangjam Leikai pond and Loktak lake of Manipur (a North-Eastern state of India), respectively. Both the weeds were dried at room temperature and powdered. Further, both the powdered weeds were pre-treated separately using 4% w/v NaOH solution as per the methodology of da Silva et al. (2018).

2.7.2. Saccharification of pre-treated aquatic weeds

Free cellulase and AuNPs-immobilized cellulase were added into 1 g of untreated and alkali (4% w/v NaOH) pre-treated *A. philoxeroides* and *B. mutica* biomass (pre-soaked in 100 mL of 0.1 M sodium citrate buffer; pH – 5.0). Streptomycin sulphate (0.01% w/v) was supplemented to stop any microbial contamination in the mixture. Further, polyethylene glycol (0.4% w/v) was supplemented into the mixture to stop the adverse impact of inhibitors produced (Ladeira-Ázar et al., 2019) and incubated at 45 °C under shaking conditions for 96 h. Samples were centrifuged at 6000g for 30 min and the supernatant was withdrawn at specific time interval for estimating total reducing sugar (TRS) yield.

The production of TRS (mg/g) after free cellulase and AuNPs-immobilized cellulase based hydrolysis process was quantified using DNS method (Miller, 1959). The saccharification efficiency (%) was calculated according to the equation of Mandels and Sternberg (1976):

$$\% \text{ Saccharification} = \frac{\text{Reducing sugars (mg/g)} \times 0.9}{\text{Initial substrate concentration (mg/g)}} \times 100$$

2.8. Fermentation using immobilized yeast cells-

2.8.1. Yeast culture used

Saccharomyces cerevisiae NCIM 3095 (obtained from CSIR-National Chemical Laboratory, Pune, India) was inoculated into 100 mL of sterile YEPD (yeast extract peptone dextrose) broth (yeast extract – 1 g, peptone – 2 g, dextrose – 2 g, and pH – 6.0 ± 0.2) aseptically and incubated at 30 °C for 12 h at 150 rpm in orbital shaker. After required incubation period, the yeast culture was centrifuged at 10,000g for 20 min and cells were col-

lected. Yeast cells were dissolved in sterile distilled water for further experiments.

2.8.2. Immobilization of yeast cells on sodium alginate

Sodium alginate (5% w/v) was uniformly mixed with distilled water for 72 h and then autoclaved. After cooling, the yeast cell suspension was added into sodium alginate solution and mixed uniformly using clean glass rod. Sodium alginate-yeast cells suspension was drawn in a sterile syringe and poured drop-by-drop into cold calcium chloride solution (1% w/v) to form calcium alginate beads of uniform size (5 mm). These beads were incubated in calcium chloride solution for 1 h, followed by its incubation in the sterile potassium chloride (3% w/v) solution. After 30 min, beads were filtered and then washed several times using sterile distilled water for further experimental purposes (Devi and Nagamani, 2018).

2.8.3. Simultaneous saccharification and fermentation

Free cellulase and AuNPs-immobilized cellulase were added into 1 g of untreated and NaOH pre-treated *A. philoxeroides* and *B. mutica* biomass (pre-soaked in 100 mL of 0.1 M sodium citrate buffer; pH – 5.0). After 6 h of hydrolysis at 45 °C, yeast cells immobilized in calcium alginate (8 g) were added into each of the saccharified biomass aseptically. Erlenmeyer flasks were then kept in orbital shaker at 150 rpm for 30 °C. Samples were withdrawn at 72 h for the estimation of ethanol.

2.9. Analytical assay

Ethanol content was estimated using Gas Chromatography (Agilent Model 8890) equipped with capillary column. The oven temperature was maintained at 450 °C, injection temperature at 80 °C, and ion source temperature at 120 °C. Nitrogen was used as carrier gas with a flow rate of 1.20 bar pressure.

2.10. Statistical analyses

All the experiments were performed in triplicate and data were recorded as mean \pm SD. ANOVA was implemented to analyse the significance ($P \leq 0.05$) level.

3. Results

3.1. Biosynthesis of AuNPs

The synthesis of AuNPs using cellulase as reductant was confirmed by observing the appearance of purple colour solution (Fig. 1).

3.2. Characterization of AuNPs

The biosynthesis of AuNPs was further confirmed by observing surface plasmon resonance absorption peak (λ_{\max}) at 574 nm using UV-Vis spectrum (Fig. 1). The FT-IR spectrum of the synthesized AuNPs is shown in Fig. 2. The major peaks observed at 3512, 1506, and 1158 cm^{-1} denote the strong O–H groups, C = C, and O–H groups, respectively. The zeta potential value of the AuNPs was estimated as –8 mV, indicating the stability of nanoparticles synthesized (Fig. 3a). Fig. 3b shows the DLS analysis of AuNPs in terms of size distribution Vs intensity. The graph depicts that the size of the highest percentage of AuNPs synthesized was 5–7 nm. The diffraction peaks pattern of AuNPs synthesized is shown in Fig. 3c which confirmed the face-centred cubic (fcc) structure of atomic gold crystals. The peaks corresponded to (111), (200), and (220) lattice planes of fcc gold structure. No characteristic

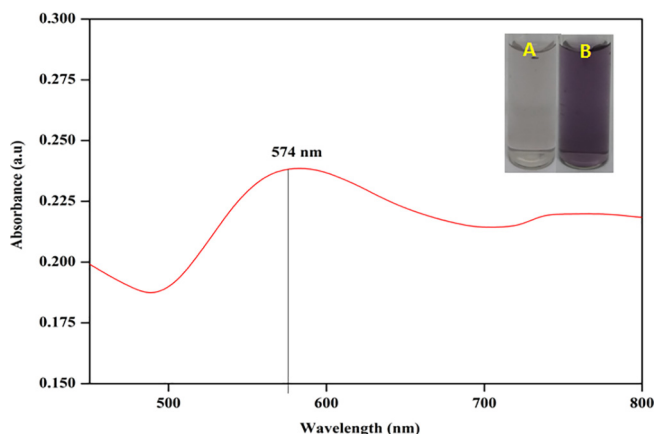


Fig. 1. Synthesis of AuNPs using cellulase, as evident by change in the colour of the solution from colourless (A) to purple (B) in colour. Synthesis of AuNPs was confirmed by observing surface plasmon resonance peak (λ_{\max}) at 574 nm using UV-Vis spectrum.

peaks of impurities were reported which showed good crystalline nature of AuNPs. The elemental composition and stoichiometry of the synthesized AuNPs are shown in Fig. 3d. The SEM image of nanoparticles revealed the synthesis of gold nanocrystals (Fig. 3e).

3.3. TRS and saccharification efficiency of *A. philoxeroides* biomass

The effect of free and AuNPs-immobilized cellulase on TRS production from untreated and 4% w/v NaOH pre-treated *A. philoxeroides* biomass is shown in Table 1A. The untreated biomass was poorly affected and estimated TRS yield of 4.45 ± 0.18 , 6.4 ± 0.17 , 8.48 ± 0.18 , 12.3 ± 0.18 , and 8.36 ± 0.2 mg/g at 12, 24, 48, 72, and 96 h of treatment, respectively using AuNPs-immobilized cellulase. The pre-treated biomass exhibited increased TRS yield of 8.5 ± 0.2 , 10.9 ± 0.2 , 14.9 ± 0.17 , 18.95 ± 0.18 , and 15.11 ± 0.17 mg/g from 12 to 96 h using AuNPs-immobilized cellulase. The saccharification ability of untreated biomass was estimated as 20.02 ± 0.7 , 28.8 ± 0.8 , 38.16 ± 0.8 , 55.35 ± 0.7 , and $37.62 \pm 0.7\%$ at 12, 24, 48, 72, and 96 h of treatment, respectively using AuNPs-immobilized cellulase. The pre-treated biomass exhibited increased saccharification degree of 38.25 ± 0.8 , 49.05 ± 0.7 , 67.05 ± 0.7 , 85.27 ± 0.8 , and $67.99 \pm 0.8\%$ from 12 to 96 h using AuNPs-immobilized cellulase (Table 1B).

3.4. TRS and saccharification efficiency of *B. mutica* biomass

The effect of free and AuNPs-immobilized cellulase on TRS production from untreated and 4% w/v NaOH pre-treated *B. mutica* biomass is shown in Table 2A. The untreated biomass exhibited TRS yield of 5.98 ± 0.18 , 7.22 ± 0.17 , 9.46 ± 0.17 , 13.58 ± 0.18 , and 8.62 ± 0.2 mg/g at 12, 24, 48, 72, and 96 h of treatment, respectively using AuNPs-immobilized cellulase. The pre-treated biomass exhibited increased TRS yield of 9.88 ± 0.18 , 12.34 ± 0.18 , 16.28 ± 0.2 , 20.98 ± 0.17 , and 16.29 ± 0.2 mg/g from 12 to 96 h using AuNPs-immobilized cellulase. The saccharification ability of untreated biomass was estimated as 26.91 ± 0.8 , 32.49 ± 0.6 , 42.57 ± 0.7 , 61.11 ± 0.8 , and $38.79 \pm 0.8\%$ at 12, 24, 48, 72, and 96 h of treatment, respectively using AuNPs-immobilized cellulase. The pre-treated biomass exhibited increased saccharification degree of 44.46 ± 0.7 , 55.53 ± 0.8 , 73.26 ± 0.7 , 94.41 ± 0.8 , and $73.3 \pm 0.7\%$ from 12 to 96 h using AuNPs-immobilized cellulase (Table 2B).

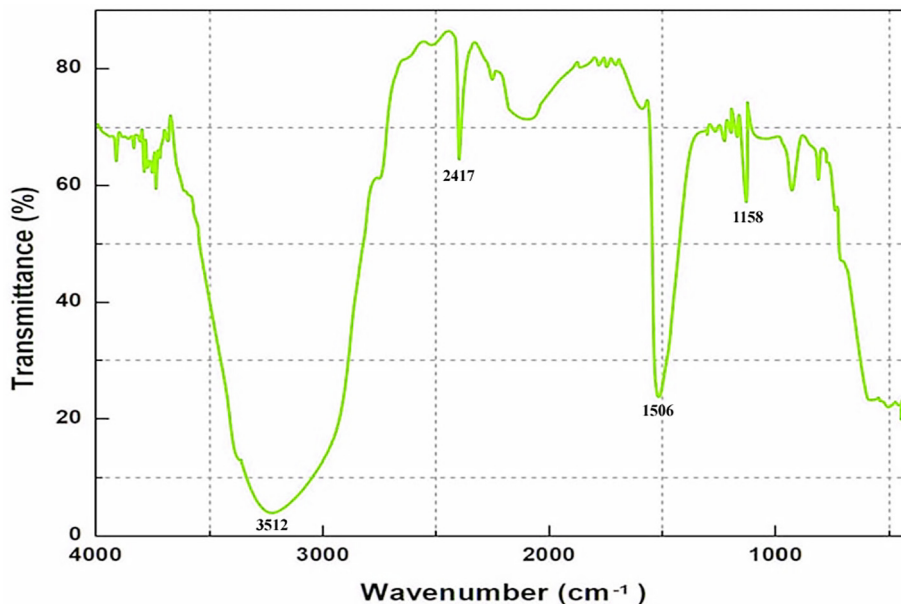


Fig. 2. FT-IR spectrum of the synthesized AuNPs.

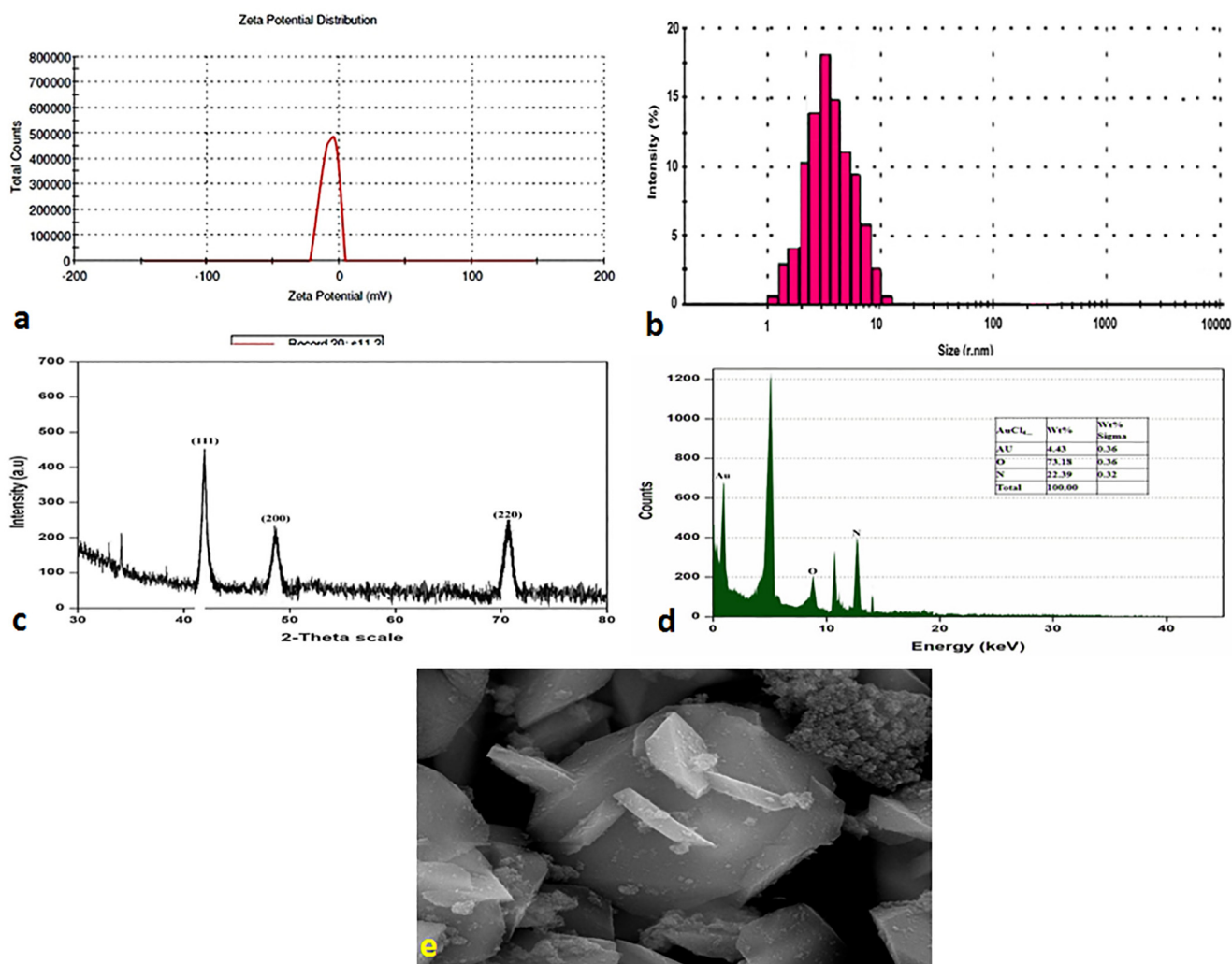


Fig. 3. (a) Zeta potential, (b) DLS, (c) XRD, (d) EDX analyses, and (e) SEM image of AuNPs [gold nanocrystals].

Table 1ATRS production (mg/g) from untreated and pre-treated *A. philoxeroides* biomass using free cellulase and AuNPs-immobilized cellulase.

Incubation period (h)	Free cellulase		AuNPs-immobilized cellulase	
	Untreated	NaOH pre-treated	Untreated	NaOH pre-treated
12	4.32 ± 0.16 ^e	8.32 ± 0.2 ^d	4.45 ± 0.18 ^d	8.5 ± 0.2 ^e
24	5.81 ± 0.2 ^d	10.12 ± 0.2 ^c	6.4 ± 0.17 ^c	10.9 ± 0.2 ^d
48	8.14 ± 0.17 ^b	13.34 ± 0.18 ^b	8.48 ± 0.18 ^b	14.9 ± 0.17 ^b
72	11.52 ± 0.16 ^a	15.98 ± 0.16 ^a	12.3 ± 0.18 ^a	18.95 ± 0.18 ^a
96	7.6 ± 0.17 ^c	13.48 ± 0.2 ^b	8.36 ± 0.2 ^b	15.11 ± 0.17 ^b

Values represent mean ± SD of experiments carried out in triplicate (n = 3).

a,b,c,d,e Means within the same column followed by different superscripts are significantly different (P < 0.05).

Table 1BSaccharification (%) of untreated and pre-treated *A. philoxeroides* biomass using free cellulase and AuNPs-immobilized cellulase.

Incubation period (h)	Free cellulase		AuNPs-immobilized cellulase	
	Untreated	NaOH pre-treated	Untreated	NaOH pre-treated
12	19.44 ± 0.8 ^d	37.44 ± 0.7 ^d	20.02 ± 0.7 ^d	38.25 ± 0.8 ^d
24	26.14 ± 0.8 ^c	45.54 ± 0.8 ^c	28.8 ± 0.8 ^c	49.05 ± 0.7 ^c
48	36.63 ± 0.7 ^b	60.03 ± 0.6 ^b	38.16 ± 0.8 ^b	67.05 ± 0.7 ^b
72	51.84 ± 0.8 ^a	71.91 ± 0.8 ^a	55.35 ± 0.7 ^a	85.27 ± 0.8 ^a
96	34.2 ± 0.7 ^b	60.66 ± 0.8 ^b	37.62 ± 0.7 ^b	67.99 ± 0.8 ^b

Values represent mean ± SD of experiments carried out in triplicate (n = 3).

a,b,c,d Means within the same column followed by different superscripts are significantly different (P < 0.05).

Table 2ATRS production (mg/g) from untreated and pre-treated *B. mutica* biomass using free cellulase and AuNPs-immobilized cellulase.

Incubation period (h)	Free cellulase		AuNPs-immobilized cellulase	
	Untreated	NaOH pre-treated	Untreated	NaOH pre-treated
12	5.82 ± 0.16 ^e	9.38 ± 0.18 ^d	5.98 ± 0.18 ^e	9.88 ± 0.18 ^d
24	6.64 ± 0.2 ^d	11.66 ± 0.2 ^c	7.22 ± 0.17 ^d	12.34 ± 0.18 ^c
48	8.94 ± 0.17 ^b	14.92 ± 0.18 ^b	9.46 ± 0.17 ^b	16.28 ± 0.2 ^b
72	12.68 ± 0.16 ^a	18.42 ± 0.16 ^a	13.58 ± 0.18 ^a	20.98 ± 0.17 ^a
96	8.1 ± 0.17 ^c	14.98 ± 0.2 ^b	8.62 ± 0.2 ^c	16.29 ± 0.2 ^b

Values represent mean ± SD of experiments carried out in triplicate (n = 3).

a,b,c,d,e Means within the same column followed by different superscripts are significantly different (P < 0.05).

Table 2BSaccharification (%) of untreated and pre-treated *B. mutica* biomass using free cellulase and AuNPs-immobilized cellulase.

Incubation period (h)	Free cellulase		AuNPs-immobilized cellulase	
	Untreated	NaOH pre-treated	Untreated	NaOH pre-treated
12	26.19 ± 0.8 ^e	42.21 ± 0.8 ^d	26.91 ± 0.8 ^e	44.46 ± 0.7 ^d
24	29.88 ± 0.6 ^d	52.47 ± 0.7 ^c	32.49 ± 0.6 ^d	55.53 ± 0.8 ^c
48	40.23 ± 0.8 ^b	67.14 ± 0.8 ^b	42.57 ± 0.7 ^b	73.26 ± 0.7 ^b
72	57.06 ± 0.6 ^a	82.89 ± 0.8 ^a	61.11 ± 0.8 ^a	94.41 ± 0.8 ^a
96	36.45 ± 0.7 ^c	67.41 ± 0.7 ^b	38.79 ± 0.8 ^c	73.3 ± 0.7 ^b

Values represent mean ± SD of experiments carried out in triplicate (n = 3).

a,b,c,d,e Means within the same column followed by different superscripts are significantly different (P < 0.05).

3.5. Ethanol estimation

The yeast cells immobilized in calcium alginate beads showed ethanol production of 45.09 and 50.1% from NaOH pre-treated *A. philoxeroides* and *B. mutica* biomass, respectively (Fig. 4).

4. Discussion

The application of cellulase in bioethanol production from lignocellulosic biomass has led researchers to develop eco-friendly and sustainable technologies (Aarti et al., 2018). As a matter of facts, these hydrolytic enzymes have opened a new avenue in bio-fuel industries. But the high cost, poor reusability, and low stability

have limited the applications of cellulolytic enzymes in cellulose based industries.

Roles of nanomaterials in the biofuel industries have provided new directions to the energy sector. Nanomaterials have the potentialities to play pivotal roles in improving bioethanol productions economically at industrial scale (Aarti et al., 2021). Nanoparticles are being used during the pre-treatment and saccharification processes not only to improve the chemistry at molecular level but also enable the specific modifications of biocatalysts (Razack et al., 2016). Metallic nanoparticles penetrate the cell wall of biomasses because of its small size and prominent interaction with the molecules to release sugars. Metallic nanoparticles are also being used to immobilize enzymes onto a support material for improved enzymatic activities (Srivastava et al., 2016). The immo-

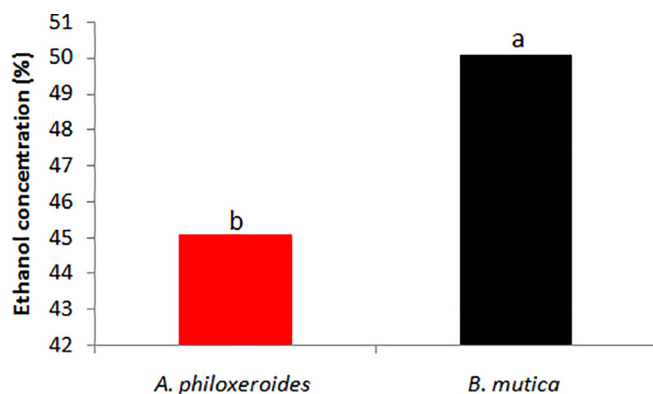


Fig. 4. Ethanol yield (%) from NaOH pre-treated (a) *A. philoxeroides* and (b) *B. mutica* biomass. ^{ab}Values with different letters are significantly ($P < 0.05$) different.

bilization of enzymes on the nanomaterials, also called as 'nanobiocatalyst' makes the process cost-effective because of high recovery and reusability at industrial scale (Mohamad et al., 2015). In fact, these nanoparticles provide large immobilization surface area to the enzyme used (Kim et al., 2006).

Over the past few years, the immobilization of enzymes in nanomaterials for biofuel production is gaining interest. Previously, metallic nanoparticles viz. Mg, Ti, Fe, Co, Fe_3O_4 , Ni, and CoPt were used for the immobilization of disparate hydrolytic enzymes (Beveridge et al., 2011). In the present investigation, AuNPs, particularly gold nanocrystals were synthesized using bacterial cellulase as reducing agent, followed by the immobilization of this cellulase on AuNPs. Cellulase immobilized on AuNPs showed improved TRS production and saccharification efficiency of NaOH pre-treated aquatic weeds biomass as compared to the free cellulase. This might be due to the reason that AuNPs provided large surface area for cellulase attachment, which led to higher enzyme loading per unit mass of nanoparticles (Grewal et al., 2017). In contrary, Mishra and Sardar (2015) synthesized AuNPs from fungal cellulase. In different studies, cellulases were immobilized on silver nanoparticles, manganese oxide nanoparticles, titanium dioxide nanoparticles, and other magnetic nanoparticles for improved properties (Husain, 2017). The immobilization of enzymes provides an increased affinity towards lignocellulosic biomass substrates, thereby causing improved hydrolysis of biomass (Xu et al., 2011). The formation of new structure due to the interaction between nanoparticles and enzymes alters the stability of the proteins. The formation of structure depends on the types of nanoparticles used for enzyme immobilization (Kirli and Kapdan, 2016).

Plethora of techniques such as diverse pre-treatment methods, enzyme hydrolysis, microbial fermentation, and recombinant yeast strains has been investigated in the past to produce bioethanol in a cost-effective manner (Bhatia et al., 2017). Many researchers demonstrated the role of β -glucosidase immobilized on metallic nanoparticles for bioethanol production (Tsai and Meyer, 2014; Alnadari et al., 2020). Cellulase immobilized on magnetic nanoparticles was used to produce bioethanol from *Sesbania aculeate* biomass and the nanobiocatalyst was recycled (Baskar et al., 2016). Similarly, *Aspergillus fumigates*-associated cellulase was immobilized on manganese oxide nanoparticles for producing bioethanol (Cherian et al., 2015). In this study, cellulase immobilized on AuNPs showed saccharification ability, followed by bioethanol production from alkali pre-treated aquatic weeds.

5. Conclusions

In summary, bacterial cellulase was used as reductant to synthesize AuNPs. The SEM analysis showed the synthesis of gold nanocrystals with an average size of 5–7 nm. Cellulase immobilized on AuNPs revealed promising rate of TRS and saccharification efficiency of *A. philoxeroides* and *B. mutica* biomass. Further, the yeast cells immobilized in calcium alginate beads showed ethanol production of 45.09 and 50.1% from NaOH pre-treated *A. philoxeroides* and *B. mutica* biomass, respectively. Findings revealed promising role of bacterial cellulase-assisted-synthesized AuNPs in saccharification, followed by successful production of bioethanol from aquatic weeds biomass effectively.

Declaration of Competing Interest

The authors declare that they have no known competing financial interests or personal relationships that could have appeared to influence the work reported in this paper.

Acknowledgement

Authors extend their appreciation to the Researchers supporting project number (RSP-2021/190), King Saud University, Riyadh, Saudi Arabia.

References

- Aarti, C., Khusro, A., Agastian, P., 2017. Goat dung as a feedstock for hyper-production of amylase from *Glutamicibacter arilaitensis* strain ALA4. *Bioresour. Bioprocess.* 4, 43. <https://doi.org/10.1186/s40643-017-0174-4>.
- Aarti, C., Khusro, A., Agastian, P., 2018. Carboxymethyl cellulase production optimization from *Glutamicibacter arilaitensis* strain ALA4 and its application in lignocellulosic waste biomass saccharification. *Prep. Biochem. Biotechnol.* 48 (9), 853–866.
- Aarti, C., Khusro, A., Agastian, P., 2021. Lignocellulosic biomass as potent feedstock resource for bioethanol production: Recent updates. *World News Nat. Sci.* 37, 164–181.
- Aarti, C., Khusro, A., Agastian, P., 2022. Saccharification of alkali pre-treated aquatic weeds biomass using partially purified cellulase immobilized on different matrices. *Biocatal. Agric. Biotechnol.* 39. <https://doi.org/10.1016/j.bcab.2022.102283>
- Agayeva, N.J., Rzayev, F.H., Gasimov, E.K., Mamedov, C.A., Ahmadov, I.S., Sadigova, N. A., Khusro, A., Al-Dhabi, N.A., Arasu, M.V., 2020. Exposure of rainbow trout (*Oncorhynchus mykiss*) to magnetite (Fe_3O_4) nanoparticles in simplified food chain: Study on ultrastructural characterization. *Saudi J. Biol. Sci.* 27 (12), 3258–3266.
- Akintelu, S.A., Yao, B., Folorunso, A.S., 2021. Bioremediation and pharmacological applications of gold nanoparticles synthesized from plant materials. *Heliyon* 7, e06591. <https://doi.org/10.1016/j.heliyon.2021.e06591>.
- Al-Dhabi, N.A., Ghilan, A.K.M., Esmail, G.A., Arasu, M.V., Duraipandiyan, V., Ponnuragan, K., 2019. Environmental friendly synthesis of silver nanomaterials from the promising *Streptomyces parvus* strain Al-Dhabi-91 recovered from the Saudi Arabian marine regions for antimicrobial and antioxidant properties. *J. Photochem. Photobiol. B: Biol.* 197, 111529.
- Alnadari, F., Xue, Y., Zhou, L., Hamed, Y.S., Taha, M., Foda, M.F., 2020. Immobilization of β -glucosidase from *Thermatoga maritima* on chitin-functionalized magnetic nanoparticle via a novel thermostable chitin-binding domain. *Sci. Rep.* 10, 1663. <https://doi.org/10.1038/s41598-019-57165-5>.
- Arasu, M.V., Arokiyaraj, S., Viayaraghavan, P., Kumar, T.S.J., Duraipandiyan, V., Al-Dhabi, N.A., Kaviyarasu, K., 2019. One step green synthesis of larvicidal, and azo dye degrading antibacterial nanoparticles by response surface methodology. *J. Photochem. Photobiol. B: Biol.* 190, 154–162.
- Baskar, G., Kumar, R.N., Melvin, X.H., Aiswarya, R., Soumya, S., 2016. *Sesbania aculeate* biomass hydrolysis using magnetic nanobiocomposite of cellulase for bioethanol production. *Renew. Energy* 98, 23–28.
- Beveridge, J.S., Stephens, J.R., Williams, M.E., 2011. The use of magnetic nanoparticles in analytical chemistry. *Annu. Rev. Anal. Chem.* 4 (1), 251–273.
- Bhatia, S.K., Kim, S.H., Yoon, J.J., Yang, Y.H., 2017. Current status and strategies for second generation biofuel production using microbial systems. *Energy Convers. Manag.* 148, 1142–1156.

- Cherian, E., Dharmendirakumar, M., Baskar, G., 2015. Immobilization of cellulase onto MnO₂ nanoparticles for bioethanol production by enhanced hydrolysis of agricultural waste. *Chinese J. Catal.* 36 (8), 1223–1229.
- Chukwuma, O.B., Rafatullah, M., Tajarudin, H.A., Ismail, N., 2020. Lignocellulolytic enzymes in biotechnological and industrial processes: a review. *Sustainability* 12, 7282. <https://doi.org/10.3390/su12187282>.
- da Silva, F.L., de Oliveira Campos, A., dos Santos, D.A., Batista Magalhães, E.R., de Macedo, G.R., dos Santos, E.S., 2018. Valorization of an agroextractive residue-Carnauba straw-for the production of bioethanol by simultaneous saccharification and fermentation (SSF). *Renew. Energy* 127, 661–669.
- Devi, N.K.D., Nagamani, A.S.S., 2018. Immobilization and estimation of activity of yeast cells by entrapment technique using different matrices. *Int. J. Pharm. Sci. Res.* 9, 3094–3099.
- Grewal, J., Ahmad, R., Khare, S.K., 2017. Development of cellulase-nanoconjugates with enhanced ionic liquid and thermal stability for *in situ* lignocellulose saccharification. *Bioresour. Technol.* 242, 236–243.
- Husain, Q., 2017. Nanomaterials immobilized cellulolytic enzymes and their industrial applications: A literature review. *JSM Biochem. Mol. Biol.* 4, 1029.
- Jayakumar, C., Magdalane, C.M., Kaviyarasu, K., Kulandainathan, M.A., Jeyaraj, B., Maaza, M., 2018. Direct electrodeposition of gold nanoparticles on glassy carbon electrode for selective determination catechol in the presence of hydroquinone. *J. Nanosci. Nanotechnol.* 18 (7), 4544–4550.
- Judy, D.A., Sherlin, Y.S., Arasu, M.V., Al-Dhabi, N.A., Choi, K.C., Bindhu, M.R., 2021. Environmental photochemistry in *Solanum trilobatum* mediated plasmonic nanoparticles as a probe for the detection of Cd²⁺ ions in water. *Environ. Res.* 202, 111918.
- Justine, M., Prabu, H.J., Johnson, I., Raj, D.M.A., Sundaram, S.J., Kaviyarasu, K., 2021. Synthesis and characterizations studies of ZnO and ZnO-SiO₂ nanocomposite for biodiesel applications. *Mater. Today: Proc.* 36, 440–446.
- Kanimozhi, K., Basha, S.K., Kaviyarasu, K., Suganthakumari, V., 2019. Salt leaching synthesis, characterization and *in vitro* cytocompatibility of chitosan/poly (vinyl alcohol)/methylcellulose-ZnO nanocomposites scaffolds using L929 fibroblast cells. *J. Nanosci. Nanotechnol.* 19 (8), 4447–4457.
- Kanimozhi, K., Basha, S.K., Kumari, V.S., Kaviyarasu, K., Maaza, M., 2018. *In vitro* cytocompatibility of chitosan/PVA/methylcellulose-Nanocellulose nanocomposites scaffolds using L929 fibroblast cells. *Appl. Surf. Sci.* 449, 574–583.
- Khusro, A., Aarti, C., Agastian, P., 2020. Microwave irradiation-based synthesis of anisotropic gold nanoplates using *Staphylococcus hominis* as reductant and its optimization for therapeutic applications. *J. Environ. Chem. Eng.* 8, <https://doi.org/10.1016/j.jece.2020.104526> 104526.
- Kim, J., Grate, J.W., Wang, P., 2006. Nanostructures for enzyme stabilization. *Chem. Eng. Sci.* 61 (3), 1017–1026.
- Kirli, B., Kapdan, I.K., 2016. Selection of microorganism immobilization particle for dark fermentative biohydrogen production by repeated batch operation. *Renew. Energy* 87, 697–702.
- Ladeira-Ázar, R.I.S., Morgan, T., Maitan-Alfenas, G.P., Guimarães, V.M., 2019. Inhibitors compounds on sugarcane bagasse saccharification: Effects of pretreatment methods and alternatives to decrease inhibition. *Appl. Biochem. Biotechnol.* 188 (1), 29–42.
- Lydia, D.E., Khusro, A., Immanuel, P., Esmail, G.A., Al-Dhabi, N.A., Arasu, M.V., 2020. Photo-activated synthesis and characterization of gold nanoparticles from *Punica granatum* L. seed oil: An assessment on antioxidant and anticancer properties for functional yoghurt nutraceuticals. *J. Photochem. Photobiol. B: Biol.* 206, <https://doi.org/10.1016/j.jphotobiol.2020.111868> 111868.
- Mandels, M., Sternberg, D., 1976. Recent advances in cellulase technology. *J. Ferment. Technol.* 54, 267–286.
- Miller, G.L., 1959. Use of dinitrosalicylic acid reagent for determination of reducing sugar. *Anal. Chem.* 31, 426–428.
- Mishra, A., Sardar, M., 2015. Cellulase assisted synthesis of nano-silver and gold: Application as immobilization matrix for biocatalysis. *Int. J. Biol. Macromol.* 77, 105–113.
- Mohamad, N.R., Marzuki, N.H.C., Buang, N.A., Huyop, F., Wahab, R.A., 2015. An overview of technologies for immobilization of enzymes and surface analysis techniques for immobilized enzymes. *Biotechnol. Biotechnol. Equip.* 29, 205–220.
- Nalini, T., Basha, S.K., Sadiq, A.M.M., Kumari, V.S., Kaviyarasu, K., 2019. Development and characterization of alginate/chitosan nanoparticulate system for hydrophobic drug encapsulation. *J. Drug Deliv. Sci. Technol.* 52, 65–72.
- Pandit, C., Roy, A., Ghotekar, S., Khusro, A., Islam, M.N., Emran, T.B., et al., 2022. Biological agents for synthesis of nanoparticles and their applications. *J. King Saud Univ. – Sci.* 34, <https://doi.org/10.1016/j.jksus.2022.101869> 101869.
- Razack, S.A., Duraiarasan, S., Mani, V., 2016. Biosynthesis of silver nanoparticle and its application in cell wall disruption to release carbohydrate and lipid from *C. vulgaris* for biofuel production. *Biotechnol. Rep.* 11, 70–76.
- Reynaldo, P.B., Adriano, E., Marcelo, M., Silvia, N., 2018. Enzymatic hydrolysis of sugarcane biomass and heat integration as enhancers of ethanol production. *J. Renew. Mater.* 6, 183–194.
- Sathiyaraj, S., Suriyakala, G., Gandhi, A.D., Babujanathanam, R., Almaary, K.S., Chen, T.W., et al., 2021. Biosynthesis, characterization, and antibacterial activity of gold nanoparticles. *J. Infect. Public Health* 14, 1842–1847.
- Shah, V., Dobiasova, P., Baldrian, P., Nerud, F., Kumar, A., Seal, S., 2010. Influence of iron and copper nanoparticle powder on the production of lignocelluloses degrading enzymes in the fungus *Trametes versicolor*. *J. Hazard. Mater.* 178, 1141–1145.
- Singhvi, M., Kim, B.S., 2020. Current developments in lignocellulosic biomass conversion into biofuels using nanobiotechnology approach. *Energies* 13, 5300. <https://doi.org/10.3390/en13205300>.
- Srivastava, N., Srivastava, M., Mishra, P.K., Ramteke, P.W., 2016. Application of ZnO nanoparticles for improving the thermal and pH stability of crude cellulase obtained from *Aspergillus fumigates* AA001. *Front. Microbiol.* 7, 9. <https://doi.org/10.3389/fmicb.2016.00514>.
- Tsai, C.T., Meyer, A.S., 2014. Enzymatic cellulose hydrolysis: Enzyme reusability and visualization of beta-glucosidase immobilized in calcium alginate. *Molecules* 19, 19390–19406.
- Xu, J., Huo, S., Yuan, Z., Zhang, Y., Xu, H., Guo, Y., et al., 2011. Characterization of direct cellulase immobilization with superparamagnetic nanoparticles. *Biocatal. Biotransform.* 29, 71–76.